DELFT UNIVERSITY OF TECHNOLOGY

DEPARTMENT OF AEROSPACE ENGINEERING

Report LR-279

TONGUE-SHAPED CRACK EXTENSION DURING FATIGUE OF HIGH STRENGTH ALUMINIUM ALLOYS

by

J.A. Vlasveld and J. Schijve

DELFT - THE NETHERLANDS

April 1979

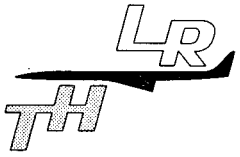

DELFT UNIVERSITY OF TECHNOLOGY

DEPARTMENT OF AEROSPACE ENGINEERING

Report LR-279

TONGUE-SHAPED CRACK EXTENSION DURING FATIGUE OF HIGH STRENGTH ALUMINIUM ALLOYS

by

J.A. Vlasveld and J. Schijve

DELFT - THE NETHERLANDS

April 1979

ABSTRACT

Fracture surfaces of both service and laboratory fatigue fractures frequently show dark tongue-shaped marks. In fatigue tests on 7075-T6 specimens such tongues were produced by high peak loads. Measurements indicated that a tongue is not formed during a single burst of crack extension but is the result of a number of successive pop-ins requiring an increasing load. Therefore tongue formation is a quasi-stable phenomenon. The tunnelling fracture in the centre of plate thickness is accompanied by unfailed ligaments at the plate surfaces which reduce the stress intensity at the crack tip. The effect of different material conditions and loading direction on tongue forming was studied. A Dugdale-type model was developed to describe the growth of a tongue. The model was in good agreement with the various test results.
The analysis of the problem has some relevance to validity requirements for K_{Ic}. A formula pertaining to tongues proposed by Forsyth was slightly modified and found to be approximately correct for the present results.

NOTATIONS

a_i, σ_i, K_i	crack length, stress and K at initiation of tongue
a_{max}, σ_{max}, K_{max}	ditto at end of tongue
Δa	$a_{max} - a_i$
C	width correction factor
COD	crack opening displacement
K_ℓ	K due to ligament stresses
L	longitudinal direction
ℓ	length of crack front
P	load
T	transverse direction
t	thickness
W	specimen width
α	slope factor (eq. 2)
1 MN/m^2	= 154.04 psi = 0.1020 kgf/mm^2
1 $MN/m^{3/2}$	= 910.05 psi $\sqrt{in}$ = 3.2246 $kgf/mm^{3/2}$

CONTENTS

1. INTRODUCTION

Fatigue fractures in high strength aluminiumalloys frequently show dark tongue-shaped parts interspersed between more brigthly reflecting bands. An example of a service failure is shown in Figure 1 and fracture surfaces of laboratory specimens with similar features are presented in Figure 2. Crack propagation tests reported by Hudson and Hardrath in 1963 (Ref. 1) clearly indicated that high peak loads caused these tongue shaped crack extensions. Several observations referred to in the literature are summarized below:

1. Tongues can be produced in a single cycle. Crack extension in the centre of the plate thickness is larger than at the plate surfaces, where the crack front trails behind (tunnelling) (Refs. 1, 2).
2. Tongues represent ductile crack extensions. When viewed through an electron microscope the fracture surface of a tongue shows dimples formed during the rupture process (Ref. 2). The process is very much similar to pop-in during fracture toughness tests.
3. The tendency for tunnelling depends on the type of alloy. The 7075-T6 alloy is wellknown for exhibiting tongues whereas the extent of tongues is smaller in the 2024-T3 alloy (Refs. 3, 4). It was also observed in the 2618 alloy (Ref. 5) and in high strength steel (Refs. 6, 7).
4. Tongues also occur in thin sheet material (in Ref. 8 for t = 2 mm), provided the crack is still in the tensile mode (Ref. 9).
5. Tongues of the same extent were found in tests in aggressive and non-agressive environments (Ref. 4).
6. The brightly reflecting part of the fracture surface succeeding the periphery of the tongue is due to fatigue load cycles and shows the well known fatigue striations (Ref. 2).
7. High peak loads usually produce significant delays in subsequent crack growth. As a result a substantial period of crack growth retardation can occur after a tongue has been formed. In this period straightening of the crack front will occur, which may lead to a new tongue during a subsequent peak load.

It is easily recognized that the state of plane stress at the material surfaces and the plane strain condition at the interior should contribute an essential part to any explanation of the above observations. In this respect the plastic zone size, the yield stress of the material and the plate thickness are significant

Unfortunately it cannot be said that the occurrence of tongues is fully understood and predictable. The present investigation was primarily carried out to explore a number of questions:

(a) Does crack extension during tongue-formation occur in a stable or an unstable way? The "pop-in" phenomenon in fracture toughness tests and the noise sometimes heard in fatigue tests suggest an unstable crack extension.

(b) Under which conditions is tongue-shaped extension initiated and why does it stop instead of proceeding catastrophically. A criterion proposed by Forsyth (Ref. 10) will be checked, but a new model based on concepts of fracture mechanics is presented.

(c) Which material characteristics are significant for the formation of tongues.

To answer these questions tests have been carried out on specimens of the 7075 alloy plate material, heat treated to different conditions. Tongues were produced in a controlled way and crack extension was measured during tongue formation. Measurements of tongue geometry were performed afterwards. Cross sections of the fractures were prepared for microscopical examination to obtain further information on the fracture mechanism. In addition some fracture surfaces produced during flight-simulation tests, made available by the National Aerospace Laboratory NLR, were analysed.

Results are presented and discussed in the following sections with a number of conclusions at the end of the paper. The present paper is mainly based on a fairly extensive thesis by the first author (Ref. 11, in Dutch).

2. ANALYSIS OF FRACTURE SURFACES FROM FLIGHT-SIMULATION LOADED SPECIMENS

In flight-simulation tests ground-air-ground transitions are applied with either gust loads or manoeuvre loads (or both) in between. Usually a variety of different flights is applied. The more severe flights contain the rarely occurring extreme loads of the load spectrum and such high loads can produce tongues. Figure 2 shows large tongues in the 7075-T6 alloy, small ones in the 2024-T3 materials and hardly any tongues in 7475-T6 alloy. The tendency to tongue-formation apparently correlates to the K_{Ic}-values. An analysis of the maximum loads applied during the severest flights which produced the tongues, indicated that the corresponding K_{max}-values were equal to or slightly exceeding estimated K_{Ic}-values. Nevertheless, complete failure did not occur. As compared to 7075-T6 the superior fracture toughness of 7475-T76 is clearly illustrated by the virtual absence of tongues on its fracture surface.

Extensive scanning electron microscopy of the fracture surfaces revealed small secondary cracks in the tongues and in the final failure part, but not in the fatigue part, unless the tests were carried out in salt water. In the latter case relatively long and narrow secondary cracks were present not only in tongues and final failure part, but also in areas formed by fatigue. Microscopical cross-section examination proved them to be branched and intercrystalline. As will be discussed later these cracks most probably originated from stress corrosion after completion of the tests.

The first type of secondary cracks, being parallel to the plate surface (XOY-plane, fig. 3), was caused by a high stress component along the crack front (σ_z). Considering the relatively small number of these cracks and the fact that their average size was smaller than the estimated plastic zone size (plane strain) it is believed that these cracks did hardly affect the state of stress. It is concluded that secondary cracks are not of special importance to tongue-shaped

crack extension. The high K_{Ic}-value for 7475-T76 should be explained by the absence of intermetallics (Ref. 12) rather than by some kind of small scale delamination.

Transmission electron microscopy confirmed the presence of dimples in the tongues, typical for ductile rupture.

Another remarkable observation can be made in Figure 2. The tongues on the 7075-T6 specimen show a tendency to form a double peaked crack front. Shortly before the first large tongue is formed one can even observe two small separate tongues at about 1/3 and 2/3 of the thickness. Chemical analysis over the thickness of the plate indicated small but systematic inhomogeneities (see Figure 4) with minima of the main alloying elements in the centre of the plate. This corresponded to a lower hardness at mid thickness while certain differences between the microscopical material structures were found also. Similar observations were made on the 7075-T6 material (t = 12.7 mm) mentioned. In Ref. 13 H.F. de Jong studied this inhomogeneity in thickness direction in 25.4 mm thick 7075-T651. He made the same observations and showed that K_c-values from specimens taken from the centre of the plate were systematically higher than for specimens located more closely to the plate surfaces. In other words: a larger crack extension resistance was found in the centre. This explains why the tongues in Fig. 2 could show a double peak.

3. TESTS WITH CONTROLLED TONGUE FORMATION

Materials and specimens

Centre cracked specimens as shown in Fig. 3 were made of 7075 aluminium alloy bare plate materials with thicknesses of 6.35 mm and 12.7 mm respectively. The 6.35 mm material was tested in three conditions in order to study tongue forming in the same alloy for different material properties. The conditions were:

- as received (T651);
- stretched (4% plastic strain);
- overaged (T7).

Overaging was obtained by giving the as-received material a full new heat treatment (1 hr 480°C, water quench to 5.7°C, 3 percent stretch, ageing 6 hrs 107°C followed by 8 hrs 117°C). Static properties (rolling direction) were:

Thickness (mm)	Condition	$\sigma_{0.2}$ MN/m^2	$\sigma_{ult.}$ MN/m^2	Elongation (50 mm gage length)
12.7	As received	467	561	17.3
6.35	As received	509	584	11.8
	As received + 4% strain	585	598	9.6
	Overaged	450	518	12.6

Testing procedures

All tests were carried out in laboratory air at ambient temperature, using a closed-loop electrohydraulic Amsler machine with a maximum capacity of 200 kN. Tongue shaped crack extensions were obtained by applying peak loads in a constant-amplitude fatigue test. The various load sequences are shown in Figure 5. The frequency of the fatigue cycles was 16 to 20 Hz and the stress ratio 0.5. Most peak loads in

series I and II were applied with a constant loading rate varying from 0.3 to 2.2 MN/m^2 per second. For some peak loads in series I a constant deformation rate of 16.7 μm/sec was adopted which approximately corresponds to 0.4 MN/m^2 per second. In test series III the peak load sequence was applied automatically by a computer controlled program with sinusoidal peak load cycles at a frequency of 0.05 Hz. In test series I and II the number of peak loads in each test was small, whereas a larger number of peak loads occurred in test series III.

Two methods were adopted for observations on crack extension during a peak load cycle. A small COD meter was employed to obtain load - COD records on an X-Y plotter. An example of such a plot is shown in Figure 6. Usually the COD meter was attached to the specimen at a distance of 2 mm behind the crack tip. The second method is based on electrical potential measurements (Ref. 14). A constant electrical current through the specimen (current density 0.035 A/mm^2) induces a potential drop (V_a) between points A1 and A2 at either side of the crack (Fig. 4) and a reference potential drop (V_0) between points A_3 and A_4. During a normal crack propagation test the crack length is directly obtained from the computer, based on the ratio V_a/V_0 and a calibrated relation with crack length. During several peak loads, V_a and P were recorded as a function of time, see Figure 7 for an example.

Test results

An important result is illustrated by the records shown in Figures 6 and 7. Crack extension during a peak load apparently occurred in a series of small steps, indicating successive fast pop-ins. Obviously the extension did not happen in a single unstable burst. During peak-loading creaking noises could be heard.

Tongue shaped crack extension (tunnelling) usually occurred without any visible crack growth at the plate surfaces. However, after high peak loads butterfly shaped zones of plastic deformation were easily visible (Fig. 8). If the specimen was pulled to failure some stable

crack extension in one of the butterfly regions was observed, indicating a tendency towards shear lip formation. After a further increase of load the specimen fractured completely in an unstable way.

Peak loads produced the wellknown delay effects in subsequent fatigue cycles. This will not be discussed here any further.

The first discontinuity in the COD-P record, indicating the first pop-in under increasing load, proved to coincide with (of follow very close on) the initiation of crack extension as indicated by the change in potential drop V_a across the crack. From this load at first pop-in the corresponding K-value was calculated. Results are plotted in Figure 9 as a function of K_{max} of the preceding fatigue cycles. Fractography showed that in the thicker material (t = 12.7 mm) the crack front sometimes was fairly curved while in other cases the front was at an oblique angle with the specimen surfaces. This behaviour was not found for the first peak load on a specimen, but it could happen afterwards due to inhomogeneous delay effects of the first peak load. Nevertheless Figure 9 suggests two systematic trends, which are:

(1) An increasing K for first pop-in for increasing K_{max} of the preceding fatigue cycles.

(2) A lower K for first pop-in if the material is loaded in transverse direction.

More information on subsequent pop-ins was obtained from records as shown in Figures 6 and 7. The following observations were made:

(3) A smaller number of larger crack increments was found for specimens loaded in the transverse direction as compared to specimens of the same material loaded in the longitudinal direction.

(4) The 6.35 mm material aged to the T7 condition showed a different behaviour, i.e. the potential drop records were characterized by a more gradual increase of V_a, while crack extension was almost soundless.

These two observations can also be interpreted as a more continuous

crack extension during tongue formation in the T7 material.

Macro-factography

All fracture surfaces gave clear evidence of tongues. Illustrations are shown in Figures 10, 11 and 12. The fracture surface in the tongues was irregular with a dark colour. Electron microscopy revealed the characteristic dimpled surface caused by ductile rupture. The fatigue parts of the fracture surfaces were faceted and brightly reflecting. Where fatigue crack growth had been fast the surface was more irregular and dull, especially in the centre of the thickness.

The shape of the tongue was clearly affected by loading direction and material condition. For the specimens shown in Fig. 10 the same peak load was applied at equal crack lengths (i.e.: the same K-value applied). Fig. 11 shows fracture surfaces of specimens of series III, loaded at regular intervals with equal peak loads. These pictures indicate the following trends:

a) Larger tongues are obtained if the material is loaded in transverse direction (Fig. 10).
b) The tongues are also larger if the yield strength of the material is higher (Fig. 10).
c) When comparing tongue-shaped crack extensions of the same length Δa the front of the tongue is more blunt (or: the front width is larger) if the material is loaded in the transverse direction than when loaded longitudinally (Fig. 11).
d) The same applies if the yield strength is higher (Fig. 11) and if the plate thickness is larger (compare Fig. 10 with Fig. 12).

In agreement with the above observations tongue-shaped crack extension initiates at a smaller crack length (lower K-value) if the material is loaded in the transverse direction or if the yield strength is higher.

Microscopical observations

Tongue-shaped crack extension implies a tunnelling fracture with unfractured ligaments between the tongue and the two plate surfaces. Sections through the tongue area were prepared for optical microscopy in order to get some more information on deformations and fracture in the ligaments and the tongues. In addition fracture surfaces were examined through an optical stereo-microscope. Two types of secondary cracks, parallel to the sheet surface, were observed. The first type occurred in the tongue area, in the directly following fatigue area and in the final fracture part. Crack opening was hardly detectable. Cross-section examination showed that the cracks were intercrystalline and that they were not continuous over the fracture (see Fig. 13a, centre of fracture).
It was definitely ascertained that such cracks, which were observed through the stereo-microscope some time after completion of the tests, could not be observed immediately after the test. All evidence suggests that this type of secondary cracks is due to stress corrosion in air of normal humidity and high residual stresses in the Z-direction. This is confirmed by the fact that the cracks were not found in the material aged to the T7 condition (compare Figures 13a and b).

The second type of secondary cracks was relatively short, but contrary to the first type these cracks were opened, which implies plastic deformation. Two such cracks, visible in Fig. 13a at the left of the fracture, are shown in more detail in Fig. 14. Apparently such cracks are continuous over the main fracture. They were present both in the tongues and in the final fracture area. In one of the 12.7 mm thick specimens a tongue was initiated from a spark machined slot. Initiation took place at a relatively high K-value and in the resulting tongue the secondary cracks were clearly more abundant than in comparable tongues, initiated at lower K-values from fatigue cracks. Apparently the cracks are caused during extension of the main crack by the corresponding high stresses in the Z-direction.

This type of secondary cracks was intergranular too.

The cross-sections in Figs. 13a and b were partially made through the unfractured ligaments. At the vertical boundaries of the cross-sections some lateral contraction can be observed, similar to the necking observed in Fig. 14.

4. DISCUSSION

Stress intensity at initiation of crack extension

An observation of prime importance for understanding tongue-shaped crack extension is that tongues are formed during increasing load in a number of small steps. For the ductile material (7075-T7) it was an almost continuous process, whereas for the low ductility materials it consisted of a number of small unstable crack growth increments. However, also in the latter case it required an increasing load for more steps. The observation techniques employed clearly indicated that a tongue is not a single burst of crack extension. On the contrary, the tongue forming process apparently was a quasi-stable phenomenon. In fact it is stable ductile tearing, while small instabilities can occur as a consequence of inhomogeneities in the material.
Unstable tongues can be produced if the initiation is hampered by special conditions. This was obtained in one specimen which was provided with a narrow spark-machined slit instead of a fatigue crack. A peak load caused in one single burst a tongue-shaped crack extension which was fully similar to a tongue originating from a fatigue crack (see Fig. 12). The same maximum load applied to both tongues, but the fatigue crack initiated tongue started to grow at a much lower load.

Two relevant questions now are:

(i) Under which conditions will a tongue be initiated at a fatigue crack?

(ii) Which conditions will dictate the extent of the tongue after a certain load increase?

The most simple case is a straight crack front perpendicular to the sheet surfaces. The K-value will then be representative for stress and strain intensity around the crack tip as long as the plastic zone is relatively small. The ASTM standard for fracture toughness tests requires a minimum material thickness (t) for a valid K_{Ic}, which is equal to $t = 2.5 \, (K_{Ic}/\sigma_{0.2})^2$.

In the present tests the K-value at which the first pop-in was noted is in the order of 30 $MN/m^{3/2}$ (Fig. 19) and $\sigma_{0.2}$ is in the order of 500 MN/m^2. This leads to t = 9 mm, while thicknesses of 12.7 mm and 6.35 mm were used. The ASTM requirement is not satisfied for the last thickness. However, the requirement is rather severe and it may well be assumed that plane strain conditions still prevailed along the central part of the crack front. Near the plate surfaces the material will deform under plane stress conditions, but there is no reason to see why that should affect the initiation of crack extension in the central part under plane strain. Such an influence should only by noticeable after some crack extension.

It was already suggested by Steigerwald and Hanna (Ref. 6) that extension of a fatigue crack under subsequent static loading should start at a critical value of the stress intensity factor (K_i). They came to this conclusion by test results of five different types of alloyed steels and a titanium alloy. Even more important, they found this K_i value to be independent of material thickness. Steigerwald and Hanna suggest that K_i should be approximately equal to K_{Ic}. The ASTM standard for calculating K_{Ic} requires a 2 percent crack extension. Since this is a rather small amount it seems reasonable that K_{Ic} should also be characteristic for the initiation of a tongue in thinner material.

The results in Figure 9 indicate a similar value for K at first pop-in for the 6.35 mm and 12.7 mm material. This is in agreement with the above reasoning. It further shows that K at first pop-in is lower for the transversely loaded material. This trend agrees with the general finding that K_{Ic} values for loading in the transverse direction are lower than for loading in the longitudinal direction. Figure 9 also illustrates that higher K-values at first pop-in are found for higher K_{max}-values of the preceding fatigue cycles. This trend was reported before in the literature (Ref. 14). The results in Figure 9 are not so unambiguous as suggested by the dashed lines. The higher

K-values for first pop-in were obtained for specimens with either a more curved crack front or an oblique crack front, and this might affect the K_i-value.

In summary: as long as the plate thickness is not very small it seems reasonable that the initiation of a tongue will start at a critical value of K and that this will occur in the central part of the thickness, where plane strain conditions apply. The critical value will be approximately equal to K_{Ic}, but deviations can occur due to the conditioning of the crack tip material by the preceding cyclic strain history.

Fracture and deformations during tongue growth

The tongues observed were growing under increasing load, while leaving two unfractured ligaments between the tongue and the plate surfaces, see Figure 15. A tensile mode fracture occurs in the tongue area and plastic deformations occur in the ligaments. As a first approximation the classical explanation (see Ref. 15 e.g.) for tensile mode failure in the central part and shear lip formation at the surface applies. Under plane strain in the central part maximum shear stress is carried by planes, which are perpendicular to the plate surface (parallel to the Z-axis). Under plane stress near the surface such planes are at oblique angles to the surface. In view of the low restraint on lateral contraction (ε_z) larger strains can be accommodated before fracture occurs. Necking then leads to shear lip formation. For a tongue this implies that the fracture strain has been exceeded in the tongue area, whereas a fracture criterion is not yet satisfied in the ligaments. Evidence of this behaviour was discussed before (Figs. 8, 13 and 14).

Knott (Ref. 16) has discussed the transition from plane strain along the central part of the crack front to plane stress at the surface. He points out that σ_z does not abruptly drop to zero and consequently

there will be a part along the crack front where σ_z is still intermediate between σ_x and σ_y.
Shear producing lateral plastic deformation (ε_z) is still unlikely then. As a result a tensile mode failure has to be expected although a full plane strain situation has already been alleviated. This argument may well explain why tongues can occur in fairly thin material.

If a tongue is growing under increasing load the central part of the crack front (BB in Fig. 15) will remain under predominantly plane strain conditions. Since the growth of a tongue is a (quasi-) stable phenomenon it then should be expected that the stress intensity along the central part will be constant during this growth. It should have the same value applicable to the initiation of the tongue, which was supposed previously to be approximately equal to K_{Ic}. A constant K along the central part of the crack front, while the tongue is growing, seems to be a surprising result, but it is possible due to the effect of the unfailed ligaments. The ligaments are still carrying load, which implies a restraint on crack opening for the tongue. This argument will be used to develop a model which makes the phenomenon accessible for calculations.

A fracture mechanics model for tongue forming

Obviously tongue forming is a three-dimensional phenomenon. In view of the plane strain/plane stress transition and the curved crack front a rigorous treatment is a formidable problem. However, by some plausible simplifications it can be treated analytically. For this purpose the geometry of a growing tongue is approximated as shown in Figure 16. Starting at the tongue initiation stress σ_i from AA_1A_1A some successive steps (AB_1B_1A and AC_1C_1A) are indicated, while at the maximum stress during peak loading the boundary AD_1D_1A is reached. The central parts A_1A_1, B_1B_1, C_1C_1 and D_1D_1 are supposed to be in plane strain with K_{Ic} as the applicable stress intensity along these parts during tongue extension. The other parts are supposed to be in plane stress, but it

seems reasonable and in agreement with observations that AA_1D_1D cannot be a fully unfractures ligament. It is assumed that AD_1D becomes the ligament which is still in tact and will transmit part of the load. Similar to the Dugdale approach it will be assumed that the ligaments are carrying a stress σ_y which is equal to the yield stress $\sigma_{0.2}$ and this will reduce the stress intensity along the (partly imaginary) crack front DD (Fig. 17).

For the boundary line A_1D_1 it is assumed that the depth of penetration of plane stress at initiation (AA_1) of tongue-shaped crack extension ($K = K_{Ic}$) is equal to the plane stress plastic zone size at that moment:

$$AA_1 = \frac{1}{\pi}\left(\frac{K_{Ic}}{\sigma_{0.2}}\right)^2 \tag{1}$$

Moreover, it is assumed that after initiation the depth of plane stress penetration increases linearly with crack extension Δa. Thus:

$$v(x) = \frac{1}{\pi}\left(\frac{K_{Ic}}{\sigma_{0.2}}\right)^2 + \alpha(x - A_1) \tag{2}$$

with the slope factor α still being unknown. A value for α has been derived from the shape of a large tongue in the 12.7 mm material, where some accuracy could be expected. The flanks of the tongues of specimen 1.1 (Fig. 12) give an average slope β (= D_1D/AD) = 0.4 for Δa = 8.2 mm. For point D_1 equation (2) implies:

$$v(a_{max}) = \beta\Delta a = \frac{1}{\pi}\left(\frac{K_{Ic}}{\sigma_{0.2}}\right)^2 + \alpha\Delta a \tag{3}$$

Substitution of $\beta = 0.4$, $K_{Ic} = 30$ MN/m$^{3/2}$ (to be discussed later), $\sigma_{0.2} = 467$ MN/m^2 (measured) and $\Delta a = 0.0082$ m leads to $\alpha = 0.24$.
For the ligament width a(x) it follows with eqs. (2) and (3):

$$u(x) = \frac{v(a_{max})}{\Delta a}\,(x - a_i) = \left[\frac{1}{\pi\Delta a}\left(\frac{K_{Ic}}{\sigma_{0.2}}\right)^2 + \alpha\right](x - a_i) \tag{4}$$

The ligament load is proportional to the ligament width and it can be translated to an "effective" ligament stress σ_ℓ acting on the full thickness (Fig. 17).

$$\sigma_\ell(x) = -\frac{2u(x)}{t}\,\sigma_{0.2} \tag{5}$$

The corresponding stress intensity factor is (Ref. 17):

$$K_\ell = \int_{a_i}^{a_{max}} \frac{\sigma_\ell(x)\,dx}{\sqrt{\pi a_{max}}}\left[\sqrt{\frac{a_{max} + x}{a_{max} - x}} + \sqrt{\frac{a_{max} - x}{a_{max} + x}}\right] \tag{6}$$

A width correction factor on K_ℓ has been ignored, since it would make the integral intractable. However, it is easily shown from formulas in Ref. 17 that the correction factor for crack edge loading near the crack tip is much smaller than the Fedderson factor for a central crack. With substitution of eqs. (4) and (5) and

$$\Delta a = a_{max} - a_i \tag{7}$$

integration of eq. (6) leads to:

$$K_\ell = -\frac{4\sigma_{0.2}\sqrt{\pi a_i}}{\pi t}\left[\frac{1}{\pi}\left(\frac{K_{Ic}}{\sigma_{0.2}}\right)^2 + \alpha\Delta a\right]\left[1 + 2\,\frac{\Delta a}{a_i} - \frac{a_i}{\Delta a}\,\text{arc sec}\left(1 + \frac{\Delta a}{a_i}\right)\right]\sqrt{1 + \frac{\Delta a}{a_i}} \tag{8}$$

For the partly imaginary crack front DD superposition gives:

$$K_{DD} = K(\sigma_{max}, a_{max}) + K_\ell \;(= K_{Ic}) \tag{9}$$

and according to the basic idea of the model outlined before, this K-factor should be equal to K_{Ic}. Combining eqs. (8) and (9) finally gives:

$$\sigma_{max} = \frac{K_{Ic} + \frac{4\sigma_{0.2}\sqrt{\pi a_i}}{\pi t}\left[\frac{1}{\pi}\left(\frac{K_{Ic}}{\sigma_{0.2}}\right)^2 + \alpha\Delta a\right]\left[\sqrt{1 + 2\,\frac{\Delta a}{a_i}} - \frac{a_i}{\Delta a}\,\text{arc sec}\left(1 + \frac{\Delta a}{a_i}\right)\right]\sqrt{1 + \frac{\Delta a}{a_i}}}{\sqrt{\pi(a + \Delta a)}\,\sqrt{\sec\frac{\pi(a_i + \Delta a)}{W}}} \qquad (10)$$

The formula shows for a certain alloy (given K_{Ic} and $\sigma_{0.2}$) of a certain thickness (t) which stress (σ_{max}) is required for a certain tongue-shaped crack extension (Δa) starting from an initial crack length a_i. A value $\alpha = 0.24$ has been mentioned before, but the choice of K_{Ic} is still somewhat arbitrary. In view of the data in Figure 9 values K_{Ic} = 30 MN/m$^{3/2}$ for the longitudinal direction and K_{Ic} = 22.5 MN/m$^{3/2}$ for the transverse direction have been selected. The yield stresses adopted for both directions are 467 MN/m^2 (measured) and 450 MN/m^2 (estimated). Equation (10) is checked for the larger tongues ($\Delta a > 3$ mm), see table on page 21, which includes also data for the stress (σ_i) at which tongue initiation has started. The predicted value of σ_i is directly obtained from:

$$K_{Ic} = \sigma_i\,\sqrt{\pi a_i}\,\sqrt{\sec\frac{\pi a_i}{W}} \qquad (11)$$

The results have been plotted in Figure 18. Both the table (page 21) and the figure (black data points) show a surprisingly good agreement between prediction and test results for the maximum stress at the end of tongue forming. The error varies from -5.5 percent to +2.5 percent, with an average value of -0.7 percent. For such a simple model this is a remarkable result. For the stress at tongue initiation there is some more scatter when comparing test result with prediction, but the average error is again very small (0.4 percent). Apparently the beginning of a tongue is less well defined then the end of a tongue.

Specimen	Loading direction	a_i	Δa	σ_{max} (MN/m^2)			σ_i (MN/m^2)		
				experiment	prediction	error (%)	experiment	prediction	error (%)
1.1	L	21.2	8.2	138.7	136.9	-1.3	104.7	103.1	- 1.5
1.7		15.2	5.7	156.1	160.0	2.5	114.4	129.4	13.1
		24.8	5.5	118.6	112.1	-5.5	96.6	90.7	- 6.1
1.8		20.4	5.1	128.9	130.6	1.3	96.1	106.1	10.4
1.9		18.0	5.1	140.0	142.4	1.7	116.2	115.9	- 0.3
		26.4	3.1	100.4	99.3	1.1	86.5	85.6	- 1.0
1.3	T	9.2	4.8	157.6	149.0	-5.5	130.2	129.6	- 0.5
		21.2	10.1	111.3	112.3	0.9	88.7	77.3	-12.9
1.5		15.5	5.5	121.7	119.4	-1.9	100.2	95.6	- 4.6

The influence of the variables in eq. (10) on σ_{max} is not directly clear from the equation itself. A better appreciation can be obtained by some graphical representations. In Figure 19a the stress (σ_{max}) required for extending a tongue from three initial crack lengths is presented for material data applying to the present tests. The graphs clearly show that an initially rapid increase of σ_{max} is directly followed by an almost constant increase rate. In other words, the model predicts stable crack extension during increasing stress. Tongue extension implies an increasing ligament width, which gives an increasing restraint on crack opening and thus prevents catastrophic failure. Figure 19b shows the effect of sheet thickness which is quite large. According to the model much higher stresses are required for extension of the tongue in a thinner sheet as a result of a larger relative ligament width u(x)/t. Consequently the restraint on crack opening due to the effective ligament stress will increase. The opposite is true for a thicker sheet and it is interesting to see that for t = 25.4 mm an almost flat σ_{max} - Δa curve is obtained. Early unstable crack extension is very likely then, in agreement with general experience and recommendations for valid K_{Ic} determinations. Finally Fig. 19c shows a moderate yield stress effect (for the same K_{Ic}) and a fairly large K_{Ic} effect (for the same $\sigma_{0.2}$). In view of the model conception about tongue extension these results are easily understood.

It should be pointed out that the present model assumes a state of plane strain along a part of the crack front and therefore does not apply to very thin sheets, where at $K = K_{Ic}$ a state of plane stress already exists along the entire crack front. Also the model does not include a criterion for unstable crack extension. In a thick plate the relative ligament width and therefore K_ℓ are small (which is reflected in the flat σ_{max} - Δa curve). A limited increase in stress already produces a large tongue and causes a large increase in crack opening, i.e. large strains in the ligaments. Soon these strains can no longer be accommodated and unstable fracture occurs. In thinnner plates a much higher stress is required for such a crack extension (steeply rising

σ_{max} - Δa curve) due to the large relative ligament width (high K_ℓ). Moreover, it is possible that a state of plane stress develops along the entire crack front before final fracture occurs. Then the present model is no longer applicable.

In the present test series on the thinner plate material (t = 6.35 mm) tests were carried out for different material conditions. As a result both K_{Ic} and $\sigma_{0.2}$ were varied. Checking of equation (10) is more problematic for a few reasons. Due to the smaller thickness the tongues are smaller and the accuracy of measuring Δa should be somewhat lower while its effect on σ_{max} is larger (Fig. 19b). Secondly the slope constant α need not be exactly the same as for t = 12.7 mm, but the same value will still be adopted for some checks on equation (10). Finally also K_{Ic} is unknown, but again the K-value applicable to tongue initiation will be used. In test series II (Fig. 5) all peak loads were equal (the same maximum stress level σ_{max}) and peaks were applied at the same crack length a_i = 14.5 mm for different material conditions. Tongues produced by these peaks are used for a comparison. Since σ_{max} was the same, Δa-values were calculated with eq. (10) for this maximum stress level. The results are shown in the table below.

σ_{max} (MN/m^2)	a_i (mm)	Loading direction	Specimen	Condition	$\sigma_{0.2}$ MN/m^2	K_{Ic} MN/m$^{3/2}$	Δa (mm) observed	Δa (mm) calculated
186.7	14.5	L	5.3	T651	509	30.2	2.9	3.1
			2.2	T651 + 4% strain	585	25.9	4.8	5.0
			4.1	T7	450	32.7	2.0	1.6
		T	6.2	T651	480*	26.9	5.9	4.8
			3.1	T7	430*	28.6	3.5	3.7

* estimated values.

The agreement between prediction and experiment is fairly good again, as shown by a comparison between the last columns of the table.

Verification of Forsyth's formula

Forsyth observed tongues on the fracture surfaces of a specimen (W = 914 mm, t = 4.5 mm) of the alloy DTD 687, which is approximately similar to the alloy 7178-T6 (Refs. 10, 18, 19). The specimen was tested under constant-amplitude loading at σ_m = 96.5 MN/m^2 and σ_a = 13.8 MN/m^2 (R = 0.75) and crack growth occurred alternately by fatigue and quasi-static ductile crack extension. Tongues are sometimes observed on the fracture surfaces of fatigue fractures in 7075-T6 specimens tested with constant-amplitude loading, but only at crack lengths corresponding to the final stage of crack growth at high maximum stress intensity. Indeed the stress intensity during the test mentioned by Forsyth was relatively high (K_{max} > 23.9 MN/m$^{3/2}$); moreover, DTD 687 aged to peak hardness is a more brittle alloy ($\sigma_y \approx$ 610 MN/m^2) than 7075-T6.

Forsyth measured crack front length at initiation and at the end of tongue-shaped crack extension and he found that approximately:

$$\sqrt{a_{max}}/\ell = \text{constant} \tag{12}$$

where ℓ is the length of the crack front. His results were:

$\sqrt{a_{max}}/\ell$ = 0.66 mm$^{-1/2}$ at initiation of tongue

$\sqrt{a_{max}}/\ell$ = 0.54 mm$^{-1/2}$ at end of tongue

Forsyth argues that both initiation and end of a tongue-shaped crack extension should be considered as a matter of equilibrium of available and required energy. When the crack front length is smaller than an equilibrium length he assumes that the crack can jump to an equilibrium position by some type of brittle fracture. When the crack front length is larger than the equilibrium length the crack will grow by fatigue with striation formation. Most probably on a heuristic basis he presents

the equation:

$$\frac{\sqrt{a_{max}}}{\ell} = \frac{K_{Ic}}{1.1\ t\ \sigma_{max}\sqrt{\pi}} \tag{13}$$

This equation can also be written as:

$$\frac{1.1\ \sigma_{max}\sqrt{\pi a_{max}}}{K_{Ic}} = \frac{\ell}{t} \tag{14}$$

The origin of the factor 1.1 is not clear. In Forsyth's test a/W was smaller than 5% and the width correction on K is negligible. Dropping the factor 1.1 from eq. (14) it can be written as:

$$\frac{K(a_{max})}{K_{Ic}} = \frac{\ell}{t} \quad (\geq 1) \tag{15}$$

which is more easily understood. It says that the K-value based on a_{max} can exceed K_{Ic} provided the crack front length is larger than the thickness, i.e. for a curved crack front. For initiation of a tongue-shaped crack extension from a straight crack front ($\ell = t$ and $a = a_i$) the equation gives $K(a_i) = K_{Ic}$ in agreement with one of the basic assumptions of the present model. This model also allows to calculate ℓ as a function of $K(a_{max})$. According to eq. (15):

$$\frac{K(a_{max})}{\ell} = \frac{K_{Ic}}{\ell} = \text{constant} \tag{16}$$

It will be checked whether the model predicts this ratio to be constant for the present tests (t = 12.7 mm). According to fig. 16:

$$\ell = 2AD_1 + (t - 2DD_1) = 2\sqrt{\Delta a^2 + u(a_{max})^2} + [t - 2u(a_{max})] \tag{17}$$

$u(a_{max})$ follows from eq. (4), which gives:

$$\ell(\Delta a) = t + 2 \left\{ \sqrt{\Delta a^2 + \left[\frac{1}{\pi} \left(\frac{K_{Ic}}{\sigma_{0.2}} \right)^2 + \alpha \cdot \Delta a \right]^2} - \right.$$

$$\left. - \left[\frac{1}{\pi} \left(\frac{K_{Ic}}{\sigma_{0.2}} \right)^2 + \alpha \cdot \Delta a \right] \right\} \qquad (18)$$

With $K(a_{max}) = C \cdot \sigma_{max} \sqrt{\pi a_{max}}$, σ_{max} from eq. (10) and ℓ from eq. (18) the ratio $K(a_{max})/\ell$ (eq. (16)) can now be calculated. This has been done for the 12.7 mm thick material loaded in the longitudinal direction and a_i-values of 15, 20 and 25 mm respectively. The results indicated extremely small differences (< 0.2%) for the three a_i-values. The curve in fig. 20 shows that according to the present model the ratio $K(a_{max})/\ell$ is not constant, but the variation is relatively small. Keeping in mind the fact that the model rests on certain simplifications the results in Fig. 20 seem to support the applicability of eq. (16). As suggested by Forsyth (Ref. 10) it implies that the magnitudes of loads which caused tongue-shaped crack extensions during service failures can be deduced from the dimensions of the tongues.

Verification of eq. (16) by measurements of crack front length of tongues has been done by calculating K_{Ic} with the following equation:

$$K_{Ic} = \frac{t}{\ell} \cdot C \cdot \sigma_{max} \cdot \sqrt{\pi a_{max}} \qquad (19)$$

where all quantities in the right hand part of the equation are measured values. Such calculations were made both for initiation (a_i, σ_i) and end (a_{max}, σ_{max}) of tongue-shaped crack extension. The length ℓ of the crack front was measured with a curvimeter on enlarged pictures of the fracture surfaces. Calculated K_{Ic}-values have been plotted in Figures 21a and b. Although there is some scatter a tendency for an approximately constant K_{Ic}-value is easily observed. Moreover, any systematic difference between K_{Ic}-values calculated from crack front length and stress at initiation and end of tongue-shaped crack extention is apparently absent. The small

systematic difference of $\sqrt{a}/\ell$-values found by Forsyth for these two cases should be associated with initiation of crack extension shortly before the maximum load of the constant-amplitude cycle was reached ($\sigma_i < \sigma_{max}$).

Figures 21a and b clearly illustrate lower K_{Ic}-values for the transversely loaded specimens. Average values are presented in the table below, including results for the T6 + 4% strain and the T7 conditions. The table confirms the lower K_{Ic}-values for the transverse direction.

Thickness (mm)	Material condition	Loading direction	$K_{Ic} = \frac{t}{\ell}\sigma\sqrt{\pi a}$ (MN/m$^{3/2}$) Average	Standard deviation	Number of tongues
12.7	T651	L	29.8	6.4%	21
		T	23.1	3.0%	6
6.35	T651	L	32.6	7.5%	21
		T	26.6	5.0%	16
	T651 + 4% strain	L	26.4	3.6%	17
	T7	L	33.7	4.2%	10
		T	28.6	4.0%	12

The results of the lower thickness material indicate that a 4 percent strain, which raised the yield stress with 15%, implies a decrease of K_{Ic} with about 20 percent. Opposite effects are obtained by overaging, but the gain on K_{Ic} is not so large.

Some concluding remarks

The main goal of the present investigation was to increase our understanding of tongue-shaped crack extension, but the results do have some bearing upon the problem of "valid" fracture toughness determinations.

The COD measurements and the electropotential measurements have shown that tongues (or tunnelling) are not single explosive crack extensions. A tongue is formed during increasing load via a number of small crack growth increments. A large explosive burst will only occur if tongue initiation is difficult by some special condition at the crack tip. In the present investigation this occurred in the specimen with a spark machines thin slit. In view of these observations and the succesful model application it is thought that K_{Ic} estimates can be obtained from specimens that do not satisfy the ASTM thickness requirement. This is supported by the present results for different material conditions and different loading directions. Steigerwald and Hanna (Ref. 6) came to a similar conclusion for five different types of steel and a titanium alloy.

5. SUMMARY AND CONCLUSIONS

1) Dark tongue-shaped crack extension marks are frequently observed on fracture surfaces of both service and laboratory fatigue fractures of high strength aluminium alloy materials due to variable-amplitude loading. In the present test series on 7075 plate material (thicknesses 12.7 and 6.35 mm) many tongues were obtained by adding peak loads to a constant-amplitude loading. The dark tongue-shaped marks result from a ductile bearing rupture. Electrical potential measurements and COD measurements showed that a tongue is not produced in a single burst of crack extension as was sometimes believed. On the contrary, tongue-shaped crack extension is a progressive phenomenon, consisting of a relatively large number of small crack extensions (successive pop-ins) each requiring a further load increase. Although each small crack extension seems to occur in an unstable way the whole process is quasi stable.

2) Comparing the 7075-alloy in three different conditions (as received, overaged and as received plus 4% plastic strain) the number of small crack extensions contributing to the tongue is larger for the lower yield stress material. For the overaged material tongue-shaped crack extension was almost a continuous process. If loaded in transverse direction tongue formation occurred at lower stress levels and comprised a smaller number of larger crack increments.

3) At a straight crack front a tongue initiates when the value of the stress intensity factor reaches K_{Ic}. During further load increase two unfractured ligaments between the tongue and the plate surfaces prevent the crack from becoming unstable.

4) A Dugdale-type model was developed to analyse tongue-shaped crack extension. The ligaments are supposed to carry a stress equal to the yield stress of the material, and this restraint on crack opening reduces the stress intensity at the tip. According to the model the

criterion for extension of a tongue is a stress intensity at the tip of the tongue equal to K_{Ic}. The model was developed analytically and the formulas obtained were in remarkably good agreement with experimentally established relations. The model also produced good indications on the effects of material thickness, K_{Ic} and yield stress.

5) In the literature Forsyth proposed a relation between the maximum stress intensity factor and the crack front length (ℓ) after tongue-shaped crack extension. This relation was modified to read $K(a_{max})/K_{Ic} = \ell/t$, where a_{max} is the maximum crack length (up to the tip of the tongue) and t is the plate thickness.
According to the model this relation could well be applicable.
The modified relation was confirmed by results obtained in the present test series.

REFERENCES

1. Hudson, C.M.
   Hardrath, H.F.
   Investigation of the effects of variable-amplitude loadings on fatigue crack propagation patterns.
   NASA TN D-1803, Aug. 1963.

2. Forsyth, P.J.E.
   Ryder, D.A.
   Some results of the examination of aluminium alloy specimen fracture surfaces.
   Metallurgia, Vol. 63, 1961, pp. 117-124.

3. Schijve, J.
   Jacobs, F.A.
   Tromp, P.J.
   Flight-simulation tests on notched elements.
   Nat. Aerospace Lab. NLR, TR 74033, Febr. 1974.

4. Schijve, J.
   Jacobs, F.A.
   Tromp, P.J.
   Environmental effects on crack growth in flight-simulation tests on 2024-T3 and 7075-T6 material.
   Nat. Aerospace Lab. NLR, TR 76104, Oct. 1976.

5. Bathias, C.
   Vancon, M.
   Mechanisms of overload effect on fatigue crack propagation in aluminium alloys.
   Eng. Fract. Mech., Vol. 10, 1978, pp. 409-424.

6. Steigerwald, E.A.
   Hanna, G.L.
   Initiation of slow crack propagation in high-strength materials.
   Proc. ASTM, Vol. 62, 1962, p. 885.

7. Pearson, F.
Fatigue crack propagation experiments on vacuum remelted FV 535 steel. Roy. Aircraft Est., TR 68232, Sept. 1968.

8. Schijve, J.
Jacobs, F.A.
Tromp, P.J.
Fatigue crack growth in aluminium alloy sheet material under flight-simulation loading. Effect of design stress level and loading frequency. Nat. Aerospace Lab. NLR, TR 72018.

9. Schijve, J.
Fatigue damage accumulation and incompatible crack front orientation. Eng. Fract. Mech., Vol. 6, 1974, pp. 245-252.

10. Forsyth, P.J.E.
The causes of mixed fatigue/tensile crack growth and the significance of microscopic crack behaviour. Roy. Aircr. Est., TR 75143, Farnborough 1976.

11. Vlasveld, J.A.
Tongue shaped crack extension during fatigue (in Dutch). Thesis Department of Aerospace Eng., Delft, June 1978.

12. Kaufman, J.G.
Design of aluminum alloys for high toughness and high fatigue strength. Paper 2 in: Alloy design for fatigue and fracture resistance. AGARD-CP-185, Jan. 1976.

13. De Jong, H.F.
Variation of mechanical properties and crack growth resistance in the thickness direction of a 7075-T651 plate (in Dutch).
Dept. of Aerospace Eng., Report LR-271, July 1978.

14. Burgers, A.
Ewalds, H.L.
Van Gestel, G.F.J.A.
Vogelesang, L.B.
Crack length measurement in metal sheets with an electrical potential method (in Dutch).
Dept. of Aerospace Eng., Report VTH-194, Febr. 1975.

15. Broek, D.
Elementary engineering fracture mechanics.
Noordhoff Int. Publishing, Leiden 1974.

16. Knott, J.F.
Fundamentals of fracture mechanics.
Butterworths, London, 1973.

17. Tada, H.
Paris, P.
Irwin, G.
The stress analysis of cracks handbook.
Del Research Corp., Hellertown, 1973.

18. Forsyth, P.J.E.
Some observations and measurements on mixed fatigue/tensile crack growth in aluminium alloys.
Scripta Metallurgica, Vol. 10, 1976, p. 303.

19. Forsyth, P.J.E.
The relationship between fatigue crack behaviour and microstructure in 7178 aluminium alloy.

Roy. Aircr. Est., TR 78006,
Farnborough, 1978.

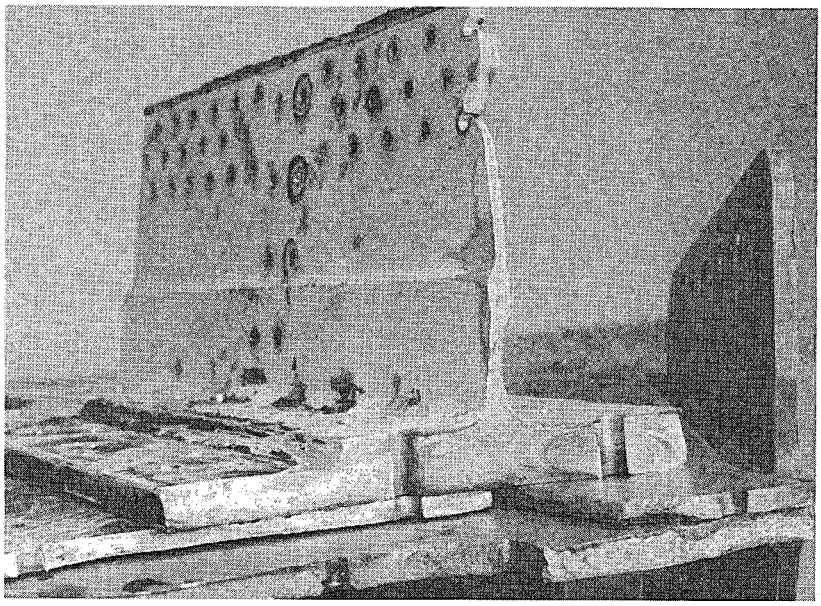

Figure 1: Tongues on fatigue failures in a lower spar cap, tension skin and strip (courtesy G.F.J.A. van Gestel, NLR).

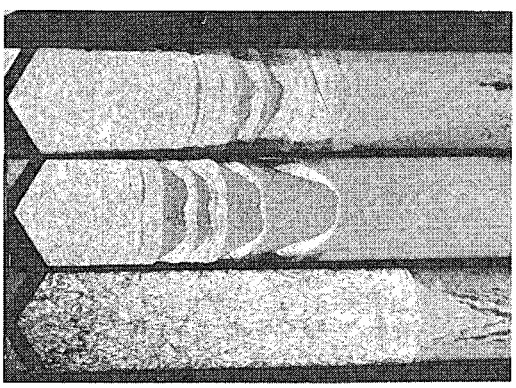

Alloy	K_{Ic} (MN/m$^{3/2}$) (literature)	σ_{max} (MN/m^2) in flight-simulation test
2024-T3	45	161
7075-T6	34	126.5
7475-T76	46.5	126.5

Figure 2: Fracture surfaces of laborarory specimens tested under flight-simulation loading (courtesy NLR).

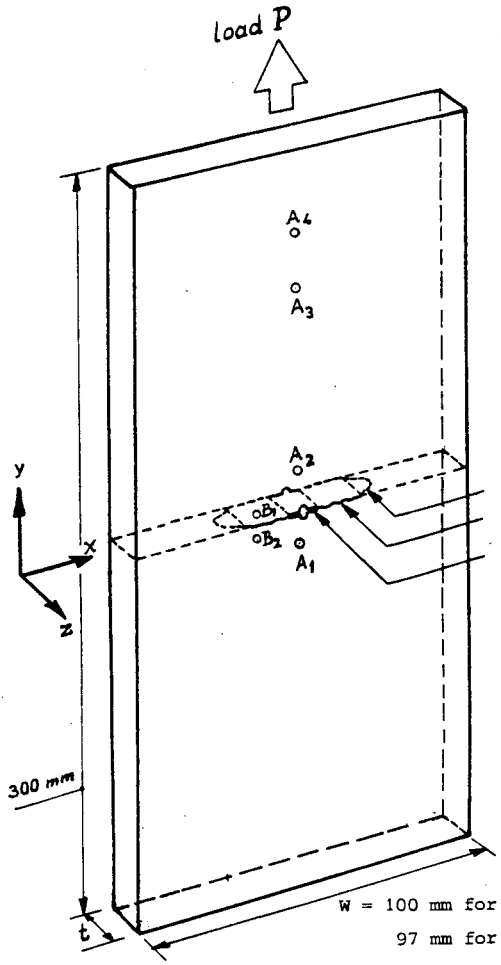

Figure 3: Specimen geometry.

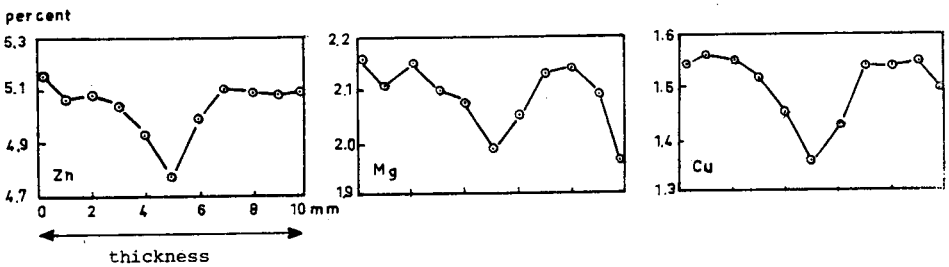

Figure 4: Inhomogeneous distribution of chemical composition in 10 mm 7075-T6 plate material.

Series	Material thickness	Load sequence (stress in MN/m^2)	Comments
I	12.7 mm	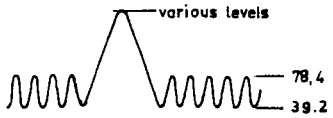	1-3 peak loads in one test 10 specimens
II	6.35 mm	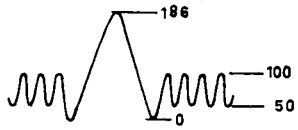	2 or 4 peaks in one test 7 specimens
III	6.35 mm	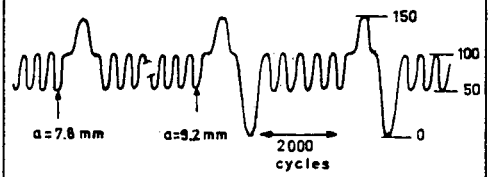	1st peak at a = 7.8 mm 2nd peak at a = 9.2 mm More peaks after every 2000 cycles 5 specimens

Figure 5: Survey of load sequences.

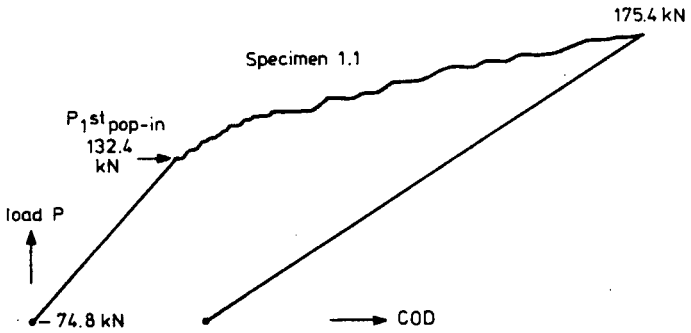

Figure 6: Load-COD record.

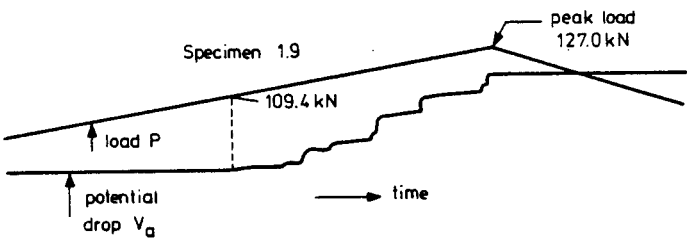

Figure 7: Recording of load and potential drop during peak load application.

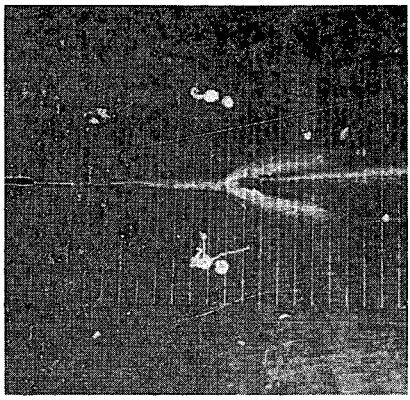

Figure 8: Butterfly plastic sones due to peak loading. Specimen tilted 15°, starter notch at left side.

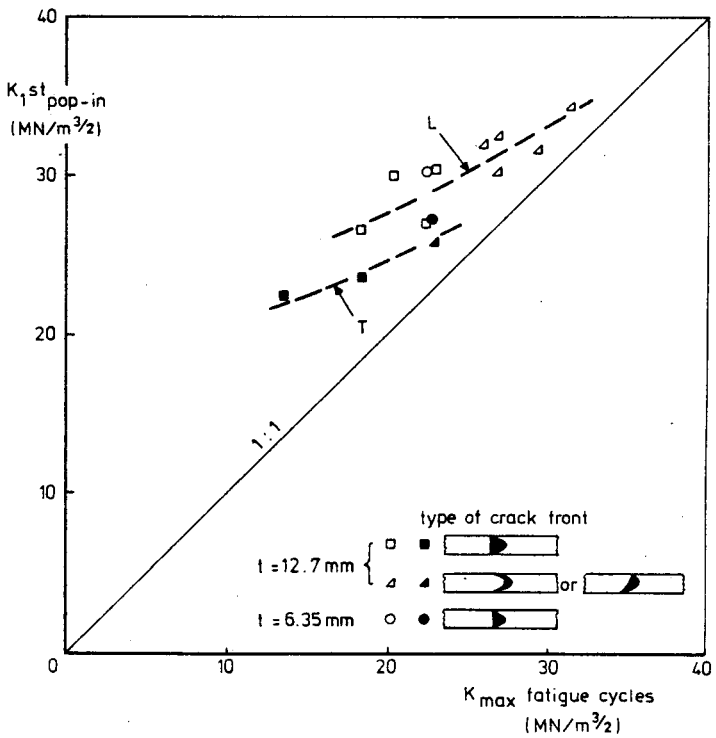

Figure 9: Effect of previous fatigue on first pop-in level for specimens loaded in longitudinal direction (L) or transverse direction (T).

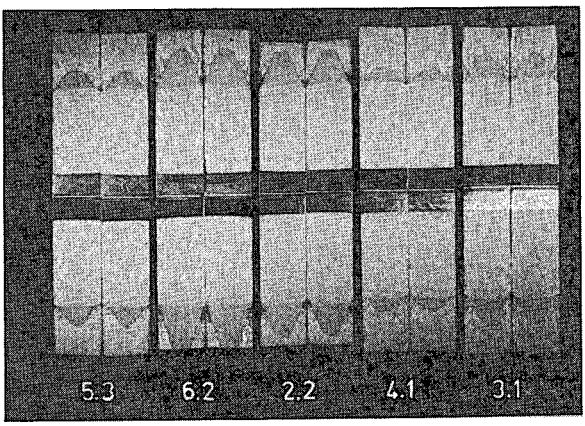

L T L L T

T651 T651 T7

+4% strain

$S_{0.2}$ = 509 585 450 MN/m^2

Material thickness 6.35 mm

Figure 10: Tongues of a single similar peak load (series II). Effect of loading direction (L or T) and material condition.

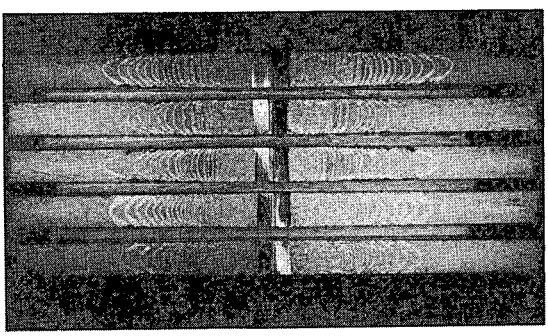

L
T651
T

L T651 + 4% strain

L
T7
T

Material thickness 6.35 mm

Figure 11: Tongues of periodic peak loads (series III). Effect of loading direction (L or T) and material condition.

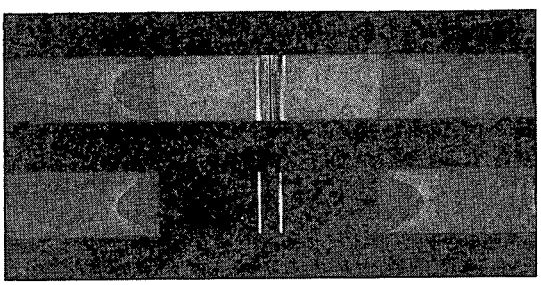

fatigue crack

spark erosion slit

Material thickness 12.7 mm
Loading direction L

Figure 12: Tongues from a fatigue crack and a sharp slit.

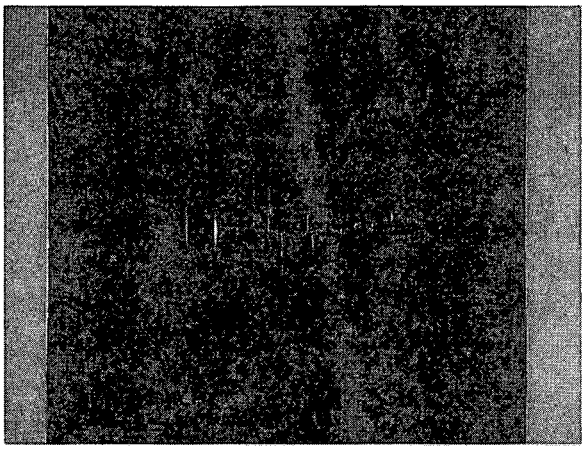

thickness = 6.35 mm

Figure 13a:
7075-T651, secondary cracks
(a ∿ 15 mm).

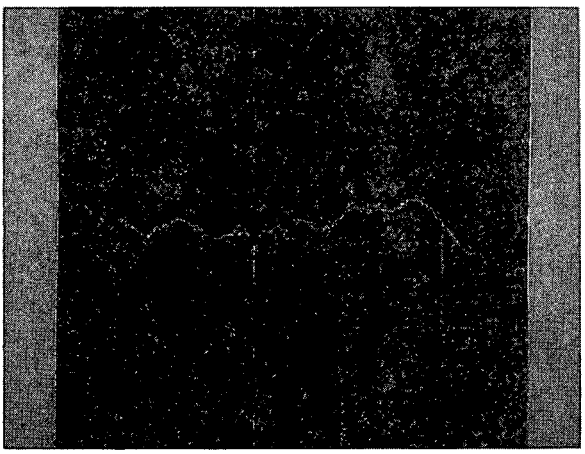

Figure 13b:
7075-T7, no secondary cracks
(a ∿ 15 mm).

Figure 13:
Cross sections (// YZ-plane)
through tongues. Dark field
illumination.

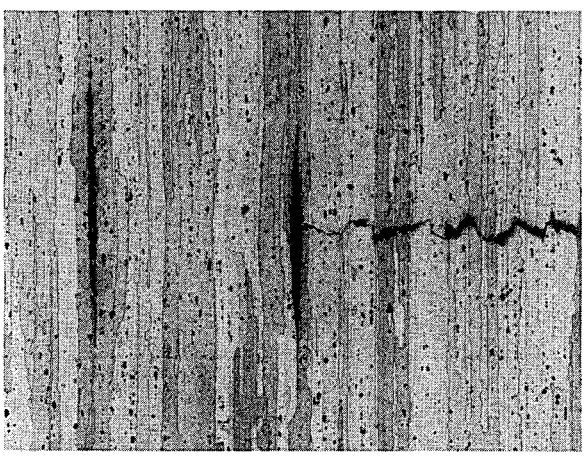

Figure 14:
Detail of Fig. 13a, inter-
crystalline secondary crac
and local necking.

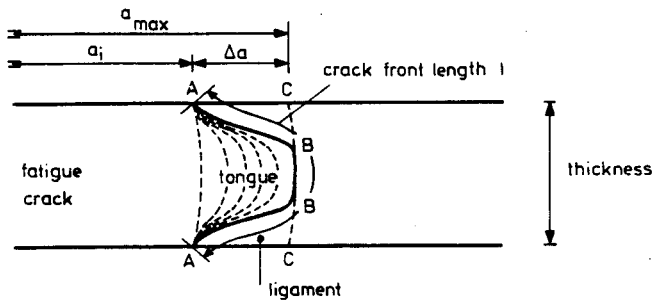

Figure 15: Schematic of tongue and ligaments.

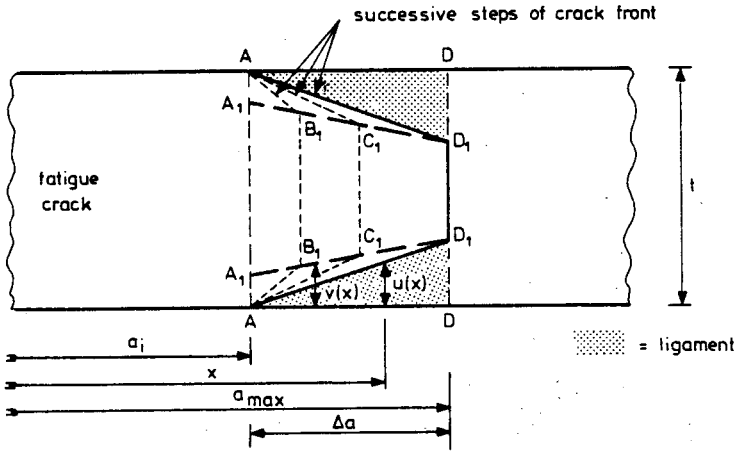

Figure 16: Schematic steps of crack front.

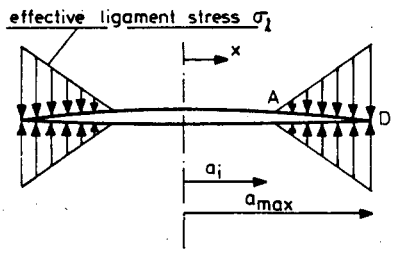

Figure 17: Dugdale approach to the ligament effect on the tip stress intensity.

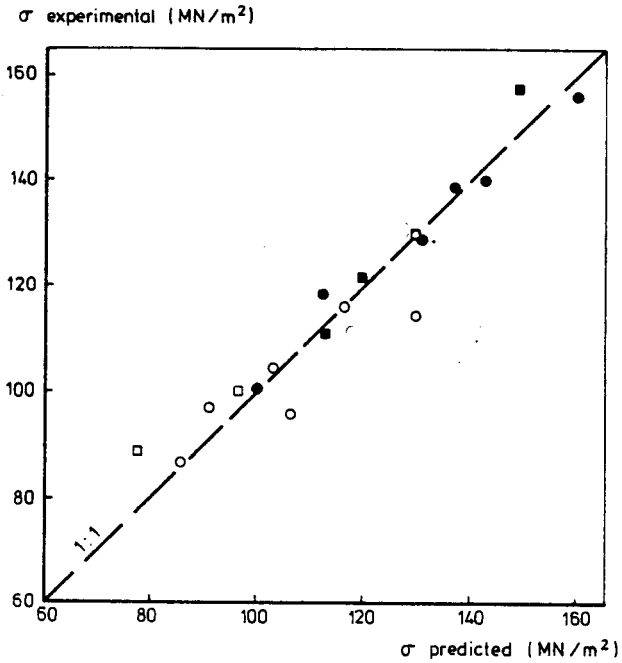

L ● } σ_{max} at end of tongue
T ■

L ○ } σ_i at initiation of tongue
T □

Figure 18: Comparison between predicted at experimental stresses at end and beginning of tongue-shaped crack extension (7075-T6, t = 12.7 mm).

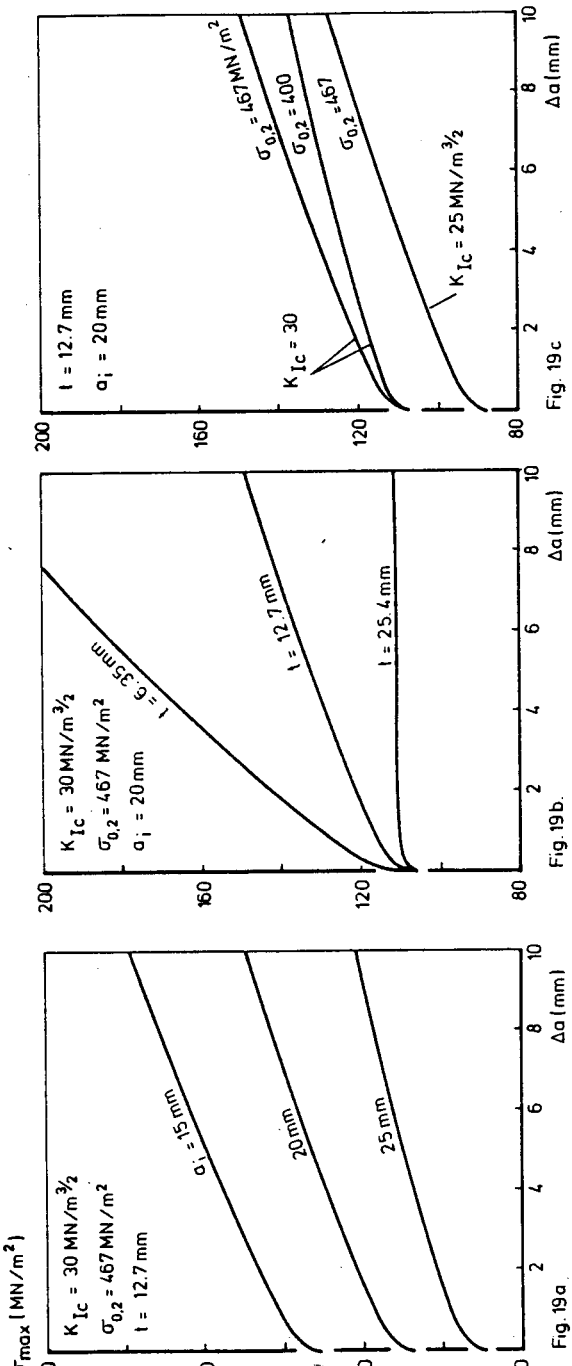

Figure 19: Increase of stress during tongue extension according to the present model (eq. 10).

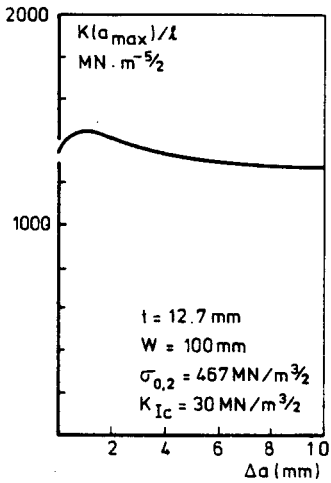

Negligible differences between curves for a_i = 15, 20 and 25 mm.

Figure 20: Calculated $K(a_{max})/\ell$ according to present model.

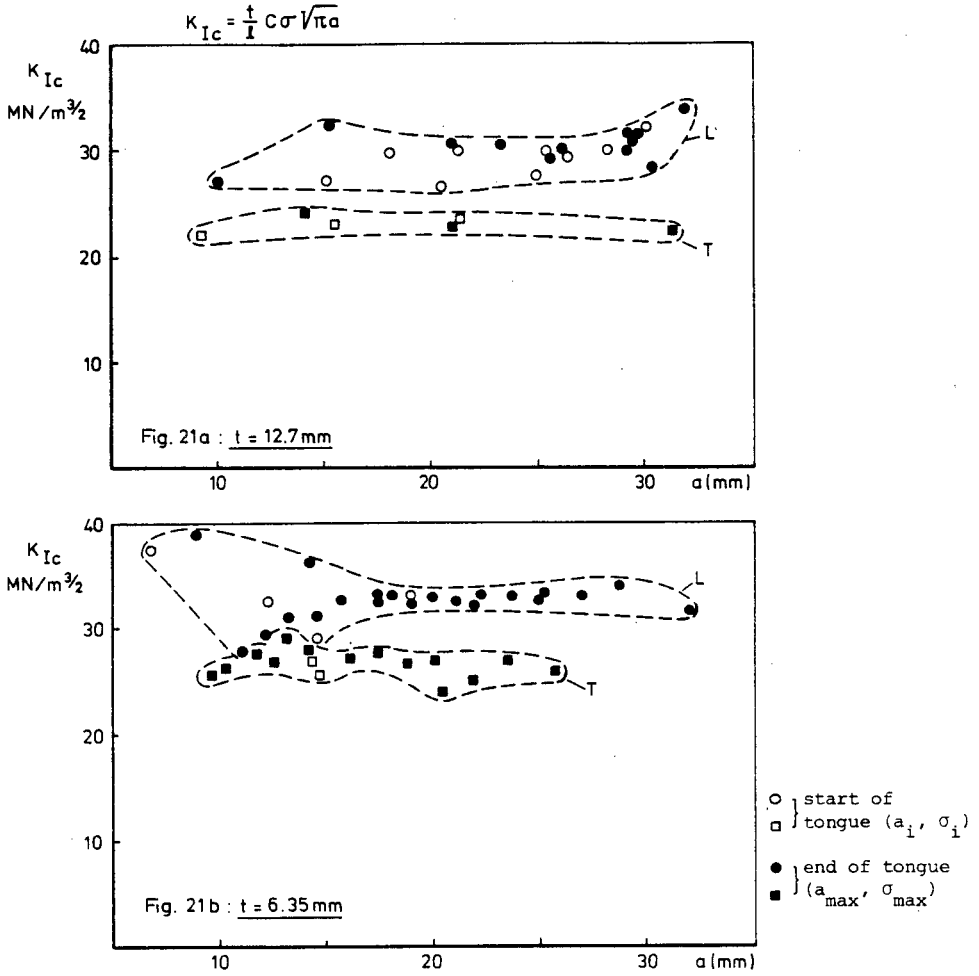

Figure 21: Calculated K_{Ic}-values (eq. 19) for 7075-Tt material.